Control Aspects of Quantum Computing Using Pure and Mixed States

Thomas Schulte-Herbrüggen*,[1] Raimund Marx,[1] Amr Fahmy,[2]
Louis Kauffman,[3] Samuel Lomonaco,[4] Navin Khaneja,[5] and Steffen J. Glaser[1]

[1] *Department of Chemistry, Technische Universität München, Lichtenbergstr. 4, D-85747 Garching, Germany*
[2] *Biological Chemistry and Molecular Pharmacology, Harvard Medical School, 240 Longwood Avenue, Boston, MA 02115, USA*
[3] *University of Illinois at Chicago, 851 S. Morgan Street, Chicago, IL 60607-7045, USA*
[4] *University of Maryland Baltimore County, 1000 Hilltop Circle, Baltimore, MD 21250, USA*
[5] *Division of Applied Sciences, Harvard University, Cambridge, MA 02138, USA*

(Dated: 2nd July 2012)

Steering quantum dynamics such that the target states solve classically hard problems is tantamount to quantum simulation and computation. And beyond, quantum control is also essential to pave the way to quantum technologies. Here, important control techniques are reviewed and presented in a unified frame covering quantum computational gate synthesis and spectroscopic state transfer alike. We emphasise that it does not matter whether the quantum states of interest are pure or not. While pure states underly the design of quantum circuits, ensemble mixtures of quantum states can be exploited in a more recent class of algorithms: it is illustrated by characterising the Jones polynomial in order to distinguish between different (classes of) knots. Further applications include Josephson elements, cavitiy grids, ion traps, NV-centres in scenarios of closed as well as open quantum systems.

Keywords: optimal quantum control, quantum computing, unitary gate design, knot theory, Jones polynomial

I. INTRODUCTION

Controlling quantum dynamics may provide access to efficiently performing computational tasks or to simulating the behaviour of other quantum systems that are beyond experimental handling themselves. In particular, quantum systems can also simulate classical systems efficiently [27, 28] sometimes even separating controllable parameters in the quantum analogue that classically cannot be tuned independently. Therefore both in simulation and computation the complexity of a problem may reduce upon going from a classical to a quantum setting [51]. On the computational end, most prominently, there is the exponential speed-up by Shor's quantum algorithm of prime factorisation [79, 80] relating to the ample class of quantum algorithms [14, 41] efficiently solving hidden subgroup problems [24, 44]. Inspired by topological quantum computation exploring braid groups, recently another type of quantum algorithm has come into focus, to wit the algorithm of Aharonov, Jones, and Landau (AJL) [5] for approximating the Jones polynomial, i.e. a central invariant in knot theory. For broader context, see also [3]. While classically it is NP-hard to distinguish two (classes of) knots in terms of their characteristic Jones polynomials, the quantum AJL algorithm, or its predecessor by Kauffman and Lomonaco (KL) [42, 43], can do so more efficiently with quantum resources. Moreover, as has been experimentally demonstrated by NMR [63, 68] , these algorithms can be implemented using thermal mixtures of quantum states. Moreover, it suffices to approximate the trace of a controlled unitary encapsulating the information of the Jones polynomial. This class of quantum algorithms is equivalent to deterministic quantum computation with one clean qubit (DQC1) [52], and actually it is even DQC1-complete [39, 78], where general belief has it that $\mathrm{P} \subsetneq \mathrm{DQC1} \subsetneq \mathrm{BQP}$, see, e.g., Ref. [78] again. As has nicely been pointed out in Ref. [68], note that DQC1 does not require the quantum bit to be in a pure state.

Since the demands for accuracy ('error-correction threshold') in quantum computation may seem daunting at the moment, the quantum simulation end is by far less sensitive. Thus simulating quantum systems [61]—in particular at phase-transitions [72]—has shifted into focus [6, 19, 36, 70].

Both quantum computation and simulation are challenging quantum engineering tasks requiring high-level manipulations of quantum dynamics. To this end, among the mathematical tools [10, 12] optimal control algorithms have been establishing themselves as indispensable tools [16, 21]. They have matured from principles [11] and early implementations [15, 69, 85] via spectroscopic applications [37, 47, 88] to advanced numerical algorithms [48, 54] for state-to-state transfer and quantum-gate synthesis [73, 76, 83] alike as will be illustrated in more detail.

On the practical end of engineering high-end quantum experiments, progress has been made in many areas including cold atoms in optical lattice potentials [9, 33], trapped ions [8, 20, 31, 32, 38, 59, 87], and superconducting qubits

* To whom correspondence should be addressed: tosh@tum.de

[18, 35, 91] to name just a few. At the interface of theory and experiment, optimal control among numerical tools have become increasingly important, see, e.g., [81] for a recent review. For instance, near time-optimal control may take pioneering realisations of solid-state qubits being promising candidates for a computation platform [13], from their fidelity-limit to the decoherence-limit [83]. More recently, open systems governed by a Markovian master equation have been addressed [73], and even smaller non-Markovian subsystems can be tackled, if they can be embedded into a larger system that in turn interacts in a Markovian way with its environment [71]. Taking the concept of decoherence-free subspaces [46, 90] to more realistic scenarios, avoiding decoherence in encoded subspaces [66] complements recent approaches of dynamic error correction [49, 50].— Along these lines, quantum control is anticipated to contribute significantly to bridging the gap between quantum principles demonstrated in pioneering experiments and high-end quantum engineering [21, 86]. Many results from controlling spin systems as can also be found in this special issue in the contributions by the groups of Laflamme at IQC or Jones in Oxford are paradigmatic for finite-dimensional quantum systems. So their implications reach far beyond spin systems and in particular beyond ensembles, which is why we first focus on the general toolbox.

To this end, the paper is structured as follows: Section II casts many of the standard quantum optimal control tasks into the framework of bilinear control systems. We show that all of them can conveniently be tackled by a unified progrmme platform DYNAMO comprising concurrent (GRAPE), sequential (KROTOV-type) as well as hybrid algorithms. In Section III, we outline a number of applications to synthesising quantum gates in closed quantum systems referring to experimental settings like Josephson charge qubits and cavitiy grids. Section IV departs from quantum circuits and shows how control applications help to distinguish classes of knots by way of their Jones polynomials. As demonstrated in Section V, also open quantum systems profit from optimal control, e.g., as a means of error avoidance.

Table I: Bilinear Quantum Control Systems

Setting and Task $\dot{X}(t) = -\big(A + \sum_j u_j(t)B_j\big)X(t)$		Drift A	Controls B_j
closed systems:			
pure-state transfer	$X(t) = \lvert\psi(t)\rangle$	iH_0	iH_j
gate synthesis (with specified global phase)	$X(t) = U(t)$	iH_0	iH_j
state transfer	$X(t) = \rho(t)$	$i\widehat{H}_0$	$i\widehat{H}_j$
gate synthesis (with free global phase)	$X(t) = \widehat{U}(t)$	$i\widehat{H}_0$	$i\widehat{H}_j$
open systems:			
state transfer	$X(t) = \rho(t)$	$i\widehat{H}_0 + \Gamma$	$i\widehat{H}_j$
quantum-map synthesis	$X(t) = F(t)$	$i\widehat{H}_0 + \Gamma$	$i\widehat{H}_j$

Here $\widehat{H}$ represents the Hamiltonian commutator superoperator represented in Liouville space.

II. ALGORITHMIC PLATFORM FOR BILINEAR QUANTUM CONTROL SYSTEMS

In practice, quantum control problems amount to steering a dynamic system such as to maximise a given figure of merit subject to the constraint of following a given equation of motion. In (finite-dimensional) quantum dynamics, the pertinent equations of motion are typically linear both in the drift as well as in the control terms, and dynamic systems of this form are known as *bilinear control systems* [22, 60, 82]

$$\dot{X}(t) = -\Big(A + \sum_{j=1}^{m} u_j(t)B_j\Big)\, X(t) \quad \text{with initial condition} \quad X_0 := X(0) \tag{1}$$

with 'state' $X(t) \in \mathbb{C}^N$, drift $A \in \mathrm{Mat}_N(\mathbb{C})$, controls $B_j \in \mathrm{Mat}_N(\mathbb{C})$, and control amplitudes $u_j(t) \in \mathbb{R}$ thus defining the $A_u(t) := A + \sum_{j=1}^{m} u_j(t)B_j$ as effective generators. Tab. I elucidates how the six standard tasks encountered in quantum optimal control take the form of bilinear control systems.

More precisely, the quality function may be expressed via the scalar product as the overlap between the final state

(or operator) of the controlled system at time T and the target state so that the common options amount to

$$f_1 := \mathrm{Re}\, g \quad \text{or} \quad f_2 := |g| \quad \text{with} \quad g := \tfrac{1}{N}\{X_{\text{target}}^\dagger X(T)\} \quad . \tag{2}$$

Define the boundary conditions as X_0, X_{target} and fix the total time T. For simplicity, we henceforth assume equal discretised time spacing $\Delta t := t_k - t_{k-1}$ for all timeslices $k = 1, 2, \ldots, M$. So $T = M\Delta t$. Then the total generator (i.e. Hamiltonian H or Lindbladian L) governing the evolution in the time interval $(t_{k-1}, t_k]$ shall be labelled by its final time t_k as

$$A_u(t_k) := A + \sum_j u_j(t_k) B_j \tag{3}$$

generating the propagator

$$X_k := e^{-\Delta t A_u(t_k)} \tag{4}$$

which governs the controlled time evolution in the timeslice $(t_{k-1}, t_k]$. Then the optimal control algorithms proceed in the following basic steps

1. *initialise* with a random (or guessed) control vector (pulse sequence) consisting of the piecewise-constant control amplitudes $u_j := \{u_j(t) \,|\, 0 \le t \le T\}$;
2. *exponentiate* $X_k = e^{-i\Delta t A_u(t_k)}$ for all $k \in$ with $A_u(t_k) := A + \sum_j u_j(t_k) B_j$;
3. *calculate forward-propagation* $X_{k:0} := X_k X_{k-1} \cdots X_1 X_0$
4. *calculate back-propagation* $\Lambda_{M+1:k+1}^\dagger := X_{\text{tar}}^\dagger X_M X_{M-1} \cdots X_{k+1}$
5. *evaluate fidelity* say $f = |g|$, where $g := \frac{1}{N} \,\mathrm{tr}\left\{\Lambda_{M+1:k+1}^\dagger X_{k:0}\right\} = \frac{1}{N} \,\mathrm{tr}\left\{X_{\text{tar}}^\dagger X_{M:0}\right\}$
6. *evaluate gradients* for all k:
   $\frac{\partial f(X(t_k))}{u_j} = \frac{1}{N} \,\mathrm{Re}\,\mathrm{tr}\left\{e^{-i\phi_g} \Lambda_{M+1:k+1}^\dagger \left(\frac{\partial X_k}{\partial u_j}\right) X_{k-1:0}\right\}$ with $\frac{\partial X_k}{\partial u_j}$ of Eqn. (5) or (6) and $e^{-i\phi_g} := g^*/|g|$;
7. *update amplitudes* for all k, e.g., by quasi-Newton $u_j^{(r+1)}(t_k) = u_j^{(r)}(t_k) + \alpha_k \,\mathcal{H}_k^{-1} \,\frac{\partial f(X(t_k))}{\partial u_j}$,
   where α_k is a suitable step size and $\mathcal{H}_k^{-1}$ is (an L-BFGS-approximation to) the inverse Hessian;
8. *re-iterate* up to terminal condition (e.g., $\frac{\partial f_k}{\partial u_j} \le f'_{\text{limit}}$ for all k).

Here the exact derivative in closed systems (or unital open systems characterised by their *normal* Lindblad generators) can be read element-wise from the eigendecomposition (with eigenvectors $|\lambda_l\rangle$ to the eigenvalues λ_ℓ)

$$\langle\lambda_l|\frac{\partial X}{\partial u_j}\lambda_m\rangle = \begin{cases} -i\Delta t \,\langle\lambda_l|B_j\lambda_m\rangle \, e^{-i\Delta t\lambda_l} & \text{if } \lambda_l = \lambda_m \\ -i\Delta t \,\langle\lambda_l|B_j\lambda_m\rangle \, \frac{e^{-i\Delta t\lambda_l} - e^{-i\Delta t\lambda_m}}{-i\Delta t\,(\lambda_l - \lambda_m)} & \text{if } \lambda_l \ne \lambda_m \ , \end{cases} \tag{5}$$

while in non-unital open systems other methods apply like

$$\frac{\partial X}{\partial u_j} \simeq -i\Delta t \; B_j \; e^{-i\Delta t A_u} \tag{6}$$

as long as the digitisation by Δt is sufficient to satisfy $\|A_u\|_2 \ll 1/\Delta t$, or one will have to resort to finite-differences etc. (see [62]). This scheme covers all the optimal control problems specified by Tab. I.

Recently we have provided a unified MATLAB-based programming frame 'DYNAMO' [62] designed in a modular way such that to the above set of bilinear control problems it embraces the different algorithmic approaches known in the literature and shown in Fig. 1. While the GRAPE algorithm (*gradient-assisted pulse engineering*) [48] updates all timeslices in the pulse sequence (control vector) *concurrently*, another type of well-established algorithms of KROTOV-type [53–55, 67, 85] do so *sequentially*. It has turned out that for optimising unitary gate synthesis for quantum information, concurrent updates of GRAPE type overtake sequential algorithms of KROTOV type well before reaching qualities in the order of the *error-correction threshold*. This is due to the fact that the recursive scheme (BFGS) to approximate the inverse Hessian pays when a constant set of time slices is updated as in GRAPE, while sequential updates preclude full profit from such recursions for second-order methods, and their first-order variants naturally loose power in the vicinity of critical points. — In the DYNAMO platform, one may also easily change between the different schemes, and the switch can actually be done on the fly during te course of an optimisation run, whenever needed to save computation time. Thus DYNAMO can readily be kept state-of-the-art with respect to future developments such as, e.g., improved preconditioning, further Newton-type algorithms, or including incoherent degrees of freedom to the control parameters.

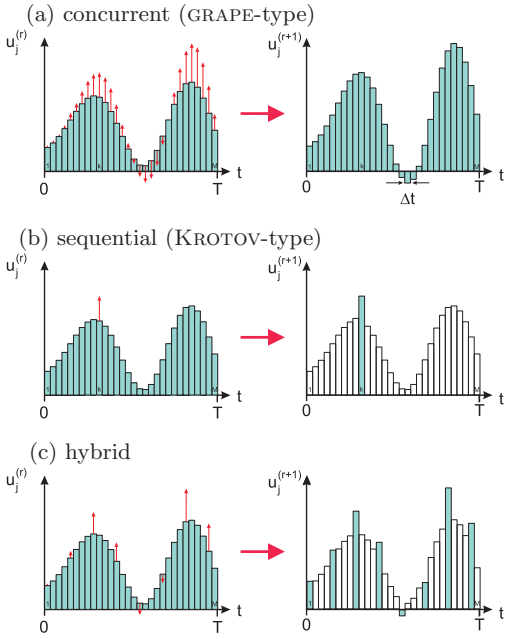

Figure 1: (Colour online) Overview on the update schemes of gradient-based optimal control algorithms unified in the DYNAMO platform. They all turn initial guesses for pulse shapes (i.e. piece-wise constant control amplitudes) into optimized shapes. In GRAPE (a) all the timeslices are updated *concurrently*. In contrast, *sequential* update schemes of KROTOV-type (b) update a single timeslice. Hybrid versions (c) can be implemented such as to update a subset of different timeslices before moving to the next (disjoint) set of timeslices. Optimizations may take total time, power, robustness, smoothness, or excitation bandwidth into account and may be executed for closed systems or open systems with known relaxation parameters.

III. APPLICATIONS IN CLOSED SYSTEMS

In order to interface theory and experiment, optimal control tools have become increasingly important [21, 74, 81]. The applications reach from ion traps via cold atoms in optical lattices to superconducting qubits [18, 35], the latter two being of particular interest to quantum electronics.

For instance, in Josephson elements we have shown how to take the pioneering realisation [89] from the fidelity limit to the decoherence limit [83]. For two capacitively coupled Josephson elements we could speed up the implementation time to realise a CNOT by a factor of five, while in three linearly coupled elements a TOFFOLI gate can be realised some 12.5 times faster than by a sequence of nine CNOT gates.

More recently, after seminal work of White [56] on exploiting auxiliary levels to speed up the synthesis of quantum gates, such a TOFFOLI gate has been implemented in a superconducting circuit by the Wallraff group [26] as elaborated on in [84]. In our case, the symmetry of the system (real symmetric Hamiltonians that can be expressed in terms σ_x and σ_z Pauli matrices) could be matched with the fact that the target CNOT gate is a square root of unity (i.e. the CNOT is self-inverse) in order to exploit optimal control to find a palindromic control sequence. Palindromic sequences can be synthesised by a cosine FOURIER series. For the experimental realisation by an electronic LCR-terminal this means the symmetry of the problem translates into Cauer synthesis without resistive components (R) as shown in all detail in [83].

On a general level, numerical optimal control lends itself to solve the *quantum compilation task* of translating quantum computational components of the high language of a unitary module into the machine language of a sequence of controlled quantum evolutions of the dynamic system given exerimentally [77]. Thus optimal control allows to depart from synthesising a unitary target only from local operations plus CNOT gates, i.e. from a restricted instruction set (RISC). Rather one may exploit precompiled few-qubit complex instruction sets (CISC) [75]. Thereby the tight error-correction threshold of RISC-computations may be relaxed to the CISC modules, which also have the advantage of being considerably faster. At the same time, we want to emphasise that the algorithms for synthesising unitary target modules are themselves entirely independent of the experimental realisation in as much as it does not matter whether the underlying experimental system operates with pure states or with ensemble mixtures [74].

As an example from cavity QED, take the paradigmatic setting of a cavity grid [34], where the qubits are arranged in the configuration of a square grid as shown in Fig. 2. Here the pair interactions between two qubits in one column

(resp. row) can be switched on and off in a fashion that only the desired qubit pair interact, while the remaining ones are left invariant. Now consider the task of implementing an indirect 1-3 quantum gate U_{13}. To this end, common wisdom would suggest the following sequential decomposition

$$U_{13} = \text{SWAP}_{23} \circ U_{12} \circ \text{SWAP}_{23} \tag{7}$$

i.e. to first SWAP qubits 2 and 3, then perform the 1-2 operation before swapping qubits 2 and 3 again. However, since there is no experimental limitation that would enforce the row and column operations to be performed sequentially, one can exploit optimal control to arrive at parallel operations which are much faster. Actually, for a variety of standard gates the speed-up against sequential decompositions varies between factors of two and nearly four (see also Tab. II as has been demonstrated in [29].

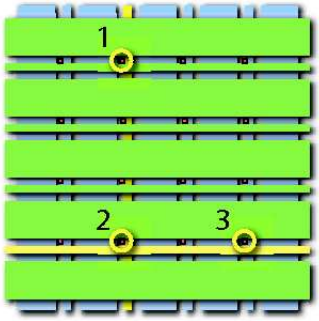

Figure 2: (Colour online) The superconducting cavity grid [34] with two layers of vertical (bottom) and horizontal (top layer) transmission line resonators coupled to qubits (small red squares). Two-qubit gates between qubits 1 and 3 are mediated indirectly via qubit 2, employing the dispersive interaction inside the two highlighted resonators.

Gate	T_{seq} $(1/J)$	T_{opt} $(1/J)$	speedup factor
iSWAP_{12}	0.5	0.5	-
CNOT_{12}	1.0	0.5	2
SWAP_{12}	1.5	0.75	2
iSWAP_{13}	3.5	1.00	3.50
CNOT_{13}	2.0	1.00	2.00
SWAP_{13}	4.5	1.15	3.91

Table II: Implementation times for a number of direct and indirect two-qubit gates in cavity grids [29]: T_{seq} is the time required for decomposing the gate into sequential two-qubit operations as in Eqn. (7); T_{opt} is the time required by the optimal control sequence. The time of $2/J$ for the sequential CNOT_{13} is special in the sense the two SWAPs can be replaced by iSWAPs [34].

IV. IMPLEMENTATION FOR 'UNTYING KNOTS BY NMR'

Many of the well-established quantum algorithms operate by solving the hidden subgroup problem in an efficient way [24, 44]. Moreover they do so by resorting to the circuit model with its experimentally challenging accuracy demands ('error-correction threshold'). In search for different and more robust classes of quantum algorithms, *topological quantum computing* with anyonic quasiparticles brought up relations to braid groups [4, 42, 45]. This is because anyonic world lines in a three-dimensional model of spacetime (consisting two spatial and one temporal dimension) form braids that can be exploited as quantum gates. These gates have the power of the circuit model with the advantage of being more robust. — When establishing the relation between topological and ordinary quantum computation, it turned out that unitary representations of braid groups useful for anyonic topological quantum computing can also be used to compute invariants of knots and links such as the Jones polynomial.

Thus there is a fruitful interplay between topological and circuit-based algorithms mediated via braid groups of knots, i.e. by unitary representations of the braid operations. In order to implement these unitaries experimentally, control aspects are of practical importance once again.

Therefore, in this section we will illustrate how thermal ensembles can be used for approximating the trace of a unitary matrix [25]. This paves the way to a recent class of quantum algorithms related to knot theory, because it allows for efficiently evaluating Jones polynomials over a range of parameters. Since knots with different Jones polynomials are clearly inequivalent (while the converse does not hold), efficient quantum algorithms determining the trace of unitaries can be of great help (in the cases distinguishable by the Jones polynomials) to solve the classically NP-hard decision problem whether two knots are equivalent in the sense they can be transformed into one another by using only Reidemeister moves and trivial moves, i.e. those which do not change the number of crossings.

More precisely, while a *knot* is defined as an embedding of the circle in three-space up to ambient isotopy, a *link* is an analogous embedding of several disjoint circles again up to isotopy. Now a *knot invariant* is any function that remains invariant under Reidemeister (and trivial) moves mentioned already. The Jones polynomial is a special form of Laurent polynomial (i.e. a polynomial with terms of both positive and negative degrees forming a ring) which itself has a degree that grows at most linearly with the number of crossings in the corresponding link. Note there is an important relation to *braid groups* established by Alexander's theorem. It says that any link can be constructed as a plat closure of some braid, namely by moving 'return' strands back into the braid, see, e.g., Ref. [78] for details.

Now the algorithm of Aharonov [2, 4, 5] takes the trace of some unitary representation of the corresponding braid group to give the Jones polynomial. Here the braid group with n strands, B_n, is generated by its $n-1$ generators representing right-handed twists $\{\sigma_1, \sigma_2, \ldots, \sigma_{n-1}\}$. For evaluating the trace, it is most convenient to exploit the connection to the Temperley-Lieb algebra [1, 3] and its unitary representation ρ by

$$\rho(\sigma_i) := A\mathbb{1} + A^{-1}U_i \quad , \tag{8}$$

where $A \in \mathbb{C}$ is of modulus one and U_i is real symmetric, while σ_i is the generator of the braid group associated to the knot of interest [92].

Next, we focus on the three-stranded braid group B_3 generated by the elements $\{\sigma_1, \sigma_2\}$. It comprises the well known standard knots *Trefoil* (up to addition of a circle disjoint from the knot), *Figure-Eight*, and the *Borromean Rings* shown in Fig. 3.

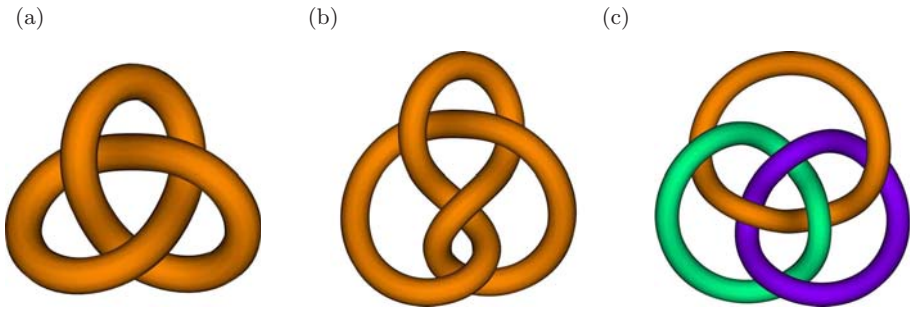

Figure 3: (Colour online) Standard knots that relate to the braid group with three strands B_3. (a) The Trefoil knot can be represented by the braid group element σ_1^3, (b) the Figure-Eight knot by $\sigma_1 \cdot \sigma_2^{-1} \cdot \sigma_1 \cdot \sigma_2^{-1}$, and (c) the Borromean rings by $\sigma_1 \cdot \sigma_2^{-1} \cdot \sigma_1 \cdot \sigma_2^{-1} \cdot \sigma_1 \cdot \sigma_2^{-1}$.

In the unitary (path model) representation of B_3 one ends up with the following unitaries that contain θ (related to the variable A of the bracket and Jones polynomial)

$$U_1 = \begin{pmatrix} e^{-i\theta} & 0 \\ 0 & -e^{i\theta}\frac{\sin(4\theta)}{\sin(2\theta)} + e^{-i\theta} \end{pmatrix} \quad \text{and} \quad U_2 := \begin{pmatrix} -e^{i\theta}\frac{\sin(6\theta)}{\sin(4\theta)} + e^{-i\theta} & -e^{i\theta}\frac{\sqrt{\sin(6\theta)\sin(2\theta)}}{\sin(4\theta)} \\ -e^{i\theta}\frac{\sqrt{\sin(6\theta)\sin(2\theta)}}{\sin(4\theta)} & -e^{i\theta}\frac{\sin(2\theta)}{\sin(4\theta)} + e^{-i\theta} \end{pmatrix} \quad . \tag{9}$$

Now, in order to get hold of the trace of U_i by a quantum measurement, we follow Ref. [25] and enlarge the quantum register by one ancilla qubit. Then the unitary U_i is translated into a controlled unitary with respect to the ancilla in the sense

$$U_i \mapsto cU_i := \begin{pmatrix} \mathbb{1}_2 & 0 \\ 0 & U_i \end{pmatrix} . \tag{10}$$

Based on the thermal ensemble state $\rho_0 \simeq \frac{1}{N}(\mathbb{1} - \frac{1}{2}\sum_k \alpha_k \sigma_{kz})$ with $\alpha_k := \frac{\hbar\omega_k}{k_B T}$, it is routine (here on the molecule chloroform by ^{1}H saturation followed by gradient filters) to prepare the suitable initial state $\rho_0 = \frac{1}{N}(\mathbb{1} - \frac{\alpha_1}{2}\sigma_{1z})$ with the z-magnetization on the natural abundance ^{13}C used as qubit. With these stipulations it is easy to proceed in three final steps

1. prepare $\rho_1 := \frac{1}{N}(\mathbb{1} - \frac{\alpha_1}{2}\sigma_{1x}) = \frac{1}{N}\mathbb{1} - \frac{\alpha_1}{2N}\begin{pmatrix} 0 & \mathbb{1}_n \\ \mathbb{1}_n & 0 \end{pmatrix}$.

2. let ρ_1 evolve under the signature sequence $cU := \prod_{\text{seq.}} cU_i$ (*vide infra*) of cU_i's specific to the knot in question. This gives the total $\rho_2 := cU\rho_1 cU^\dagger = \frac{1}{N}\mathbb{1} - \frac{\alpha_1}{2N}\begin{pmatrix} 0 & U^\dagger \\ U & 0 \end{pmatrix}$.

3. measure the expectation value of the phase sensitive ensemble detection operator [93] $D := \frac{1}{2}(\sigma_{1x} - i\sigma_{1y})$ as to give $\langle D\rangle := \mathrm{tr}\{D^\dagger \rho_2\} = -\frac{\alpha_1}{2N}\,\mathrm{tr}\,U$.

In simple cases it is well known how to translate unitary operators into NMR pulse sequences. In the more intricate case here, similar recipes apply, and backed by GRAPE, one arrives at the pulse sequences shown in Fig. 4, which are specifically designed to continuously depend on the variable θ via

$$\alpha := \frac{\pi}{2} - 2\theta \qquad \beta := \frac{\pi}{2} + \theta \qquad \gamma := \arctan\left(\frac{\cos 4\theta}{\sqrt{4\cos^2 2\theta - 1}}\right) + \frac{\pi}{2} \tag{11}$$

so that they can be implemented over a range of values of θ.

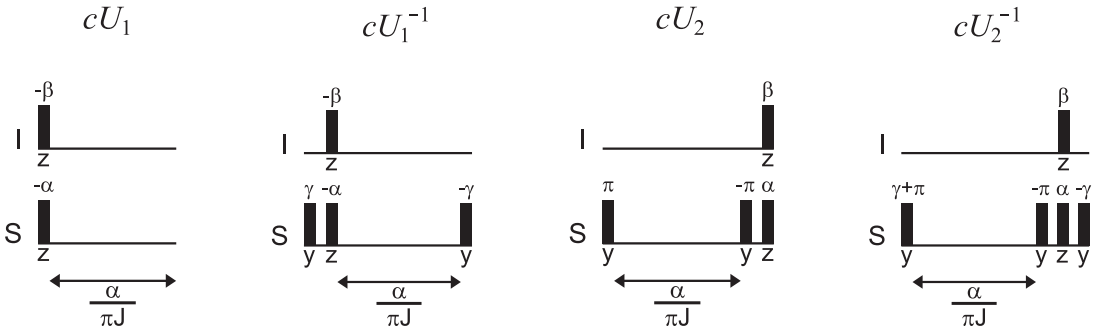

Figure 4: NMR pulse sequences implementing the set of controlled unitaries $\{cU_1, cU_1^{-1}, cU_2, cU_2^{-1}\}$ corresponding to the generators of the three-strand braid group B_3 encapsulating the Trefoil knot, the Figure-Eight knot, and the Borromean rings.

Now, for the Trefoil knot the NMR pulse sequence for cU_1 has to be applied thrice $cU_{\mathsf{tref}} := cU_1^3$, while for the Figure-Eight knot it is $cU_1 \cdot cU_2^{-1} \cdot cU_1 \cdot cU_2^{-1}$ and for the Borromean Rings $cU_1 \cdot cU_2^{-1} \cdot cU_1 \cdot cU_2^{-1} \cdot cU_1 \cdot cU_2^{-1}$ to be read from right to left to give the respective cU_{fig8} and cU_{borr}.

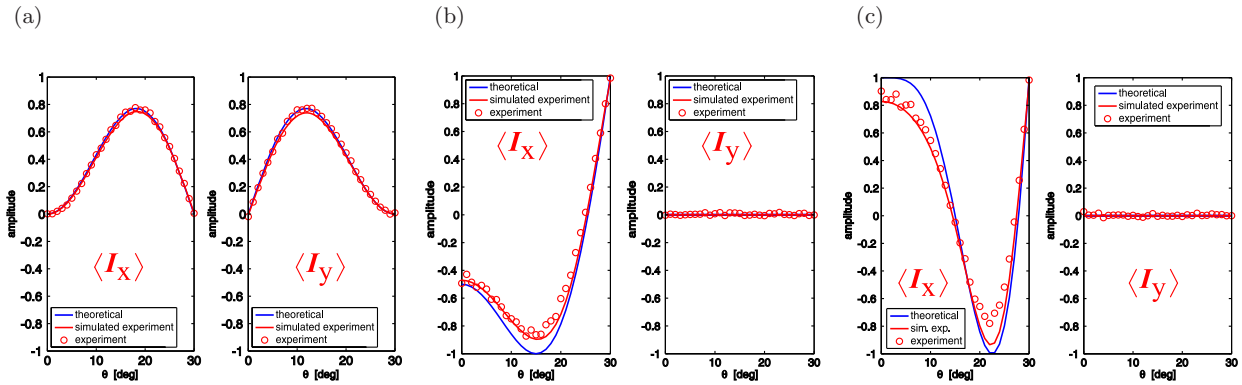

Figure 5: (Colour online) Experimental results with real parts and imaginary parts of $\frac{1}{2}\,\mathrm{tr}\{U\}$, from whence one can calculate the Jones polynomial of the various knots as functions of θ. For the Trefoil, data are given in (a), for the Figure Eight in (b), and for the Borromean rings in (c). The respective traces compare experimental results, theoretical predictions, and simulated experiments, where realisitic imperfections like relaxation, B_1-field inhomogeneity, and finite length of the pulses are included.

As shown in Fig. 5, the Jones polynomial was experimentally evaluated for each knot or link at 31 values of θ distributed over a continuous part of the domain accessible by the quantum algorithm. This readily discriminates the three-stranded knots or links by two qubits, while in Ref. [68] only single values of θ were used. Note the experimental data nicely follow the theoretical prediction and the functional dependence is so different that the predictive power of distinguishing knots or links is higher than by mere evaluation of single points.

Yet both experimental demonstrations include an evaluation of the Jones polynomial at a root of unity and thus implement a DQC1-complete quantum algorithm (see [40]). In Ref. [68], only links that contain disjoint circles were evaluated. As already mentioned, a much simpler quantum calculation using fewer qubits (here 2 qubits for a 2 strand braid representation) can calculate the Jones polynomials of the given links equally well. In contrast, the evaluations for the Figure-Eight knot and the Borromean rings cannot do with fewer than 3 strands and 2 qubits as shown in Ref. [63].

Note that even moderately intricate molecular hardware with several qubits and realistic coupling topologies goes beyond pulse sequences as easy as in Fig. 4 for the two-qubit molecule chloroform. Already the four-carbon architecture of trans-crotonic acid used in Ref. [68] required the optimal control algorithm GRAPE to be efficiently implemented experimentally. We therefore anticipate that control algorithms will play a major role even for algorithms inspired by topological quantum computation.

V. APPLICATIONS IN OPEN SYSTEMS

Controlling open systems is a particular challenge, since time-optimal controls need no longer be best adapted to cope with the specific dissipative process related to a given experimental implementation. As has been shown in more detail, the reason for this complication roots in the fact that in the controlled Lindblad master equation

$$\dot{X}(t) = -(i\widehat{H}_u + \Gamma_L)X(t) \quad \text{with} \quad \Gamma_L := \sum_k \bar{V}_k \otimes V_k - \tfrac{1}{2}\big((V_k^\dagger V_k)^t \otimes \mathbb{1} + \mathbb{1} \otimes (V_k^\dagger V_k)\big) \tag{12}$$

the generators of the dissipative part and the coherent part do not commute in the sense

$$[\widehat{H}_u, \Gamma_L] \neq 0 \quad . \tag{13}$$

It is for the same reason that many control problems in open systems are beyond algebraic tractability. On the other hand this paves the way to benefit from numerical optimal control.

In order to elucidate its power, consider the following example of a physical four-qubit system encoding two logical qubits: the starting point is the usual encoding of one logical qubit in Bell states of two physical ones

$$|0\rangle_{AB} := \tfrac{1}{\sqrt{2}}\{|01\rangle + |10\rangle\} = |\psi^+\rangle_{AB} \quad \text{and} \quad |1\rangle_{AB} := \tfrac{1}{\sqrt{2}}\{|01\rangle - |10\rangle\} = |\psi^-\rangle_{AB} \quad . \tag{14}$$

The corresonding density operators simply take the form $\rho^{\pm} := |\psi^{\pm}\rangle\langle\psi^{\pm}|$. So four density-operator elements then span a Hermitian operator subspace

$$\mathcal{B}_{AB} := \mathrm{span}_{\mathbb{R}} \{|\psi^{\pm}\rangle\langle\psi^{\pm}|\}_{AB} \quad , \tag{15}$$

that is protected against T_2-type relaxation. Clearly, an analogous subspace $\mathcal{B}_{CD}$ exists for the second logical qubit $\{|0\rangle_{CD}, |1\rangle_{CD}\}$ on the physical qubits C, D.

Henceforth we use the short hand $\mathbb{1}\mu\nu\mathbb{1} := \frac{1}{2}\mathbb{1}_2 \otimes \sigma_\mu \otimes \sigma_\nu \otimes \mathbb{1}_2$ for $\mu, \nu \in \{x, y, z, \mathbb{1}\}$. So one obtains a fully controllable system over the protected subspace of two logical qubits realised by four physical qubits, where the drift Hamiltonian reads

$$H_0 \;:=\; J_{xx}\left(xx\mathbb{1}\mathbb{1} + \mathbb{1}\mathbb{1}xx + yy\mathbb{1}\mathbb{1} + \mathbb{1}\mathbb{1}yy\right) + J_{xyz}\left(\mathbb{1}xx\mathbb{1} + \mathbb{1}yy\mathbb{1} + \mathbb{1}zz\mathbb{1}\right) \tag{16}$$

where the coupling constants are set to $J_{xx} = 2$ Hz and $J_{zz} = 1$ Hz. In the model system, the control Hamiltonians amount to the two independent (anti-phase) z-rotations

$$H_1 := z\mathbb{1}\mathbb{1}\mathbb{1} - \mathbb{1}z\mathbb{1}\mathbb{1} \quad \text{and} \quad H_2 := \mathbb{1}\mathbb{1}z\mathbb{1} - \mathbb{1}\mathbb{1}\mathbb{1}z\,. \tag{17}$$

While for both qubit pairs (AB) and (CD) the density operators $\{\rho^{\pm}_{AB}, \rho^{\pm}_{CD}\}$ form a fully controllable pair of T_2-protected logical qubits, they are not protected against (the usually much weaker) T_1-relaxation mechanisms. Now the task of finding relaxation-optimised controls implementing the target CNOT gate on the logical two qubits is highly non-trivial, because at the same time the system has to be decoupled from the Hamiltonian components of Heisenberg-type H_{XX} that otherwise would drive the protected subsystem into fast relaxing modes. In Ref. [73] we have shown that open-GRAPE produces control sequences which are some 30 times faster than Trotter-based paper-and-pen decompositions. Moreover, the controls found numerically approximate the target CNOT with a fidelity of $\geq 95\%$, while the paper-and-pen solutions would only work in the absence of T_1 processes: already T_1 relaxation as small as 1/170 of the T_2 process suffices to limit the fidelity of the paper-and-pen version to less than 15% in this example as shown in Ref. [73].

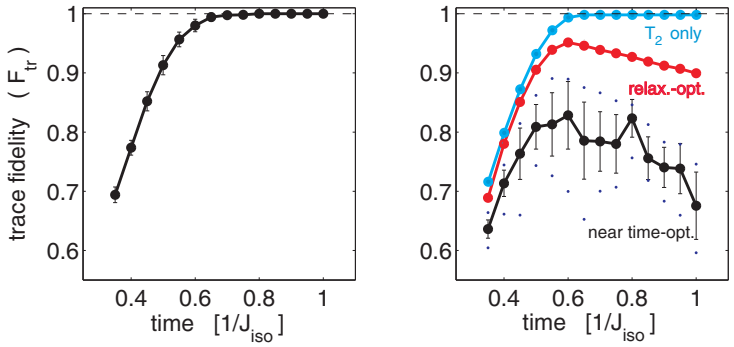

Figure 6: (Colour online) Left panel: fidelities of implementing a CNOT by the control system of Eqns. (16) and (17) versus time in the absence of relaxation (average ± rmsd over 15 independent runs). Right panel: the middle trace shows the fidelities obtained, when both T_1 and T_2 relaxation are taken into account in the optimisation by openGRAPE. Here the ratio of relxation-rate constants is $T_2^{-1} : T_1^{-1} \simeq 170 : 1$. The failure of time-optimal controls becomes evident in the lower trace: it shows the behaviour of the 15 runs optimised in the absence of relaxation (as in the left panel) when T_1 and T_2 relaxation are actually present: as expected, the qualities disperse, because some control sequences are—by serendipity—more immune to relaxation than others (mean over 15 runs with points showing the best and the worst cases), while the relaxation-optimised sequences are systematically tailored to cope with the relaxation process given in the master equation. For reference: if only T_2 relaxation processes were present, the relaxation-optimised sequences would reach full fidelity as shown in the upper trace. So the only losses of the relaxation-optimised controls are due to the weak T_1 processes.

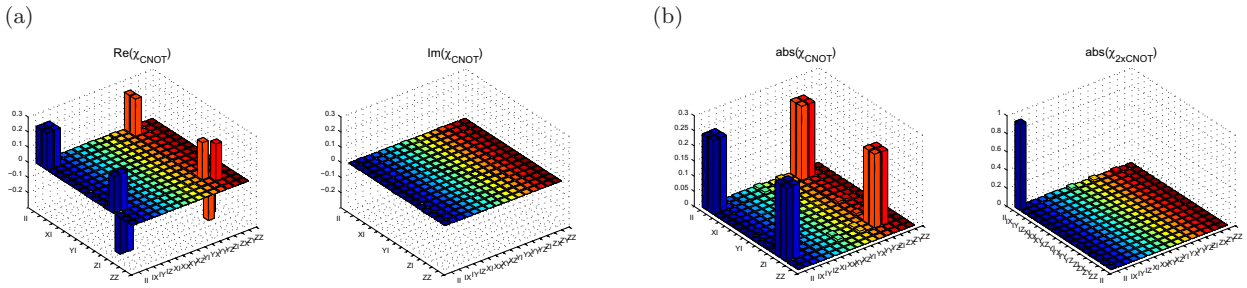

Figure 7: (Colour online) The process tomography plots for the openGRAPE-optimised CNOT gate over the T_2-protected subspace shows clean phases in (a), and its square CNOT^2 shows a nearly perfect approximation to the identity (b) as is expected for gates that are a square-root of unity.

In another instance, time-optimal control for a spin-$\frac{1}{2}$ particle in a dissipative environment has been addressed in [57, 58]. This system provides an illustrative example to show the role of singular extremals in the control of quantum systems. A simple case where the control law is explicitly determined is analysed and its optimal controls have been experimentally implemented in nuclear magnetic resonance. To our knowledge, this has been the first experimental demonstration of singular extremals in quantum systems with bounded control amplitudes.

Also for non-Markovian settings, relaxation-optimised control can be put to good use. In Ref. [71] we showed that a working qubit dissipatively interacting with a two-level fluctuator in a *non*-Markovian way, where, however, the fluctuator itself interacts with a surrounding bosonic bath in a Markovian can be treated likewise. To this end, one extends the qubit to a qubit-plus-fluctuator system, which by construction dissipates in a Markovian way so that it can be readily treated as just described above. For the task of implementing a z-gate in such a model system, the openGRAPE controls outperform conventional Rabi-based pulses by cutting the residual error (i.e. 1−fidelity) by about one order of magnitude, even if constraints like smooth pulses have to be respected for experimental reasons [71]. — Actually, the same holds on a very general scale: any non-Markovian system that can be embedded into system-plus-shell leaving only Markovian relaxation processes with the remaining bath can be tackled likewise as long as the enlarged system-plus-shell is of tractable dimensionality as expained in all detail in [73]. This idea has found further recent application in a number of standard gates [30] thus underpinning the guidelines of Tab. III drawn from [73].

Table III: Gain Potential for Relaxation-Optimised Controls *versus* Time-Optimised Controls

Category	Markovian	non-Markovian
No encoding: full Liouville space	small–medium	medium–big [71]
Encoding: protected subspace	big	difficult [94]

VI. CONCLUSIONS

We have discussed control aspects of quantum computation in a universal frame also underlying the unified programming platform DYNAMO [62]. It serves to provide concrete experimental controls for quantum computational gate synthesis or spectroscopic state transfer in general finite-dimensional control systems. The toolbox comprises the fastest among the currently known algorithms and owing to its modular structure it will be easy to keep it state-of-the-art.

Quantum gate synthesis or state transfer can thus be achieved with optimised fidelities for the experimental settings given no matter whether the implementation is meant to be via pure states or not. In a previous review [74], we have treated experimental aspects of implementing pure and pseudo-pure states in ensemble spectroscopy. Here, we have pointed out an ensemble implementation of the quantum algorithm DQC1. By characterising invariants of braid groups, it provides a bridge to topological quantum computation.

While in spin systems optimal control methods are well-established (as has become obvious by several other contributions in this issue, see also the review in Ref. [65]), here we have focussed on wider applicability by examples from Josephson elements and cavity grids, and further implementations in ion traps and NV-centres of diamonds are in progress. Most often standard decompositions into local gates plus CNOT gates are by far less robust and less efficient than the assembly of effective multi-qubits gates compiled via optimal-control. So on a very general scale, quantum opimal control can contribute a lot to exploit *error-avoidance*, thus leaving only the experimentally inevitable errors to be treated by costly *error correction* schemes. Therefore we anticipate that the control methods presented will be widely used in many further implementations of quantum simulation and quantum informationn processing including topological quantum computation. To this end, the DYNAMO package will be updated by the latest developments. This includes most recent Newton-Raphson schemes [17], filtering techniques for fast-modulating Hamiltonians [64] as well as extending the controls from coherent to encompass incoherent degrees of freedom [7]. The latter will pave the way to new classes of applications.

VII. ACKNOWLEDGEMENTS

This work was supported in part by the EU programmes QAP, Q-ESSENCE, and the exchange with COQUIT, moreover by the Bavarian excellence network ENB via the International Doctorate Programme of Excellence *Quantum Computing, Control, and Communication* (QCCC) as well as by the *Deutsche Forschungsgemeinschaft* (DFG) in the collaborative research centre SFB 631 as well as the international research group suported via the grant SCHU 1374/2-1. AF thanks NIH GM47467. Pictures for knots and links were created with KnotPlot (`http://knotplot.com/`).

VIII. REFERENCES

[1] Abramsky, S. *Mathematics of Quantum Computation and Quantum Technology*. Chapman & Hall/CRC, Boca Raton, FL, 2008, ch. Temperley-Lieb Algebra: From Knot theory to Logic and Computation via Quantum Mechanics, pp. 515–558.

[2] Aharonov, D., and Arad, I. The BQP-Hardness of Approximating the Jones Polynomial. *New J. Phys. 13* (2011), 035019.

[3] Aharonov, D., Arad, I., Eban, E., and Landau, Z. Polynomial Quantum Algorithms for Additive approximations of the Potts model and other Points of the Tutte Plane. arXiv.org/quant-ph/0702008, 2007.

[4] Aharonov, D., Jones, V., and Landau, Z. A Polynomial Quantum Algorithm for Approximating the Jones Polynomial. *Proc. 38th ACM Symp. on Theory of Computing (STOC 2006) 2006* (2006), 427 – 436.

[5] Aharonov, D., Jones, V., and Landau, Z. A Polynomial Quantum Algorithm for Approximating the Jones Polynomial . *Algorithmica 55* (2009), 395–421.

[6] Bennett, C. H., Cirac, I., Leifer, M. S., Leung, D. W., Linden, N., Popescu, S., and Vidal, G. Optimal Simulation of Two-Qubit Hamiltonians Using General Local Operations. *Phys. Rev. A 66* (2002), 012305.

[7] Bergholm, V., and Schulte-Herbrüggen, T. e-print: http://arXiv.org/pdf/1206.4945, 2012.

[8] Blatt, R., and Wineland, D. Entangled States of Trapped Atomic Ions. *Nature (London) 453* (2008), 1008–1015.

[9] Bloch, I., Dalibard, J., and Zwerger, W. Many-Body Physics with Ultracold Gases. *Rev. Mod. Phys. 80* (2008), 885–964.

[10] Brylinski, R. K., and Chen, G. *Mathematics of Quantum Computation*. Computational Mathematics Series. Chapman & Hall/CRC, Boca Raton, FL, 2002.

[11] Butkovskiy, A. G., and Samoilenko, Y. I. *Control of Quantum-Mechanical Processes and Systems*. Kluwer, Dordrecht, 1990. see also the translations from Russian originals: A. G. Butkovskiy and Yu. I. Samoilenko, Control of Quantum Systems, Part I and II, *Autom. Remote Control (USSR)* **40**, pp 485–502 and pp 629–645 (1979), as well as: A. G. Butkovskiy and Yu. I. Samoilenko, Controllability of Quantum Objects, *Dokl. Akad. Nauk. USSR* **250**, pp 22–24 (1980).

[12] Chen, G., Kauffman, L. H., and Lomonaco, S. J., Eds. *Mathematics of Quantum Computation and Quantum Technology*. Chapman & Hall/CRC, Boca Raton, FL, 2008.

[13] Clarke, J., and Wilhelm, F. Superconducting Qubits. *Nature (London) 453* (2008), 1031–1042.

[14] Cleve, R., Ekert, A., Macchiavello, C., and Mosca, M. Quantum Algorithms Revisited. *Proc. R. Soc. A. 454* (1998), 339–354.

[15] Dahleh, M., Peirce, A., and Rabitz, H. Optimal Control of Uncertain Quantum Mechanical Systems. *Phys. Rev. A 42* (1990), 1065–1079.

[16] D'Alessandro, D. *Introduction to Quantum Control and Dynamics*. Chapman & Hall/CRC, Boca Raton, 2008.

[17] de Fouquières, P. Implementing Quantum Gates by Optimal Control with Doubly Exponential Convergence. *Phys. Rev. Lett. 108* (2012), 110504.

[18] DiCarlo, L., Chow, J. M., Gambetta, J. M., Bishop, L. S., Johnson, B. R., Schuster, D. I., Majer, J., Blais, A., Frunzio, L., Girvin, S. M., and Schoelkopf, R. J. Demonstration of Two-Qubit Algorithms with a Superconducting Quantum Processor. *Nature 460* (2009), 240–244.

[19] Dodd, J. L., Nielsen, M. A., Bremner, M. J., and Thew, R. T. Universal Quantum Computation and Simulation Using Any Hamiltonian and Local Unitaries. *Phys. Rev. A 65* (2002), 040301(R).

[20] Dorner, U., Calarco, T., Zoller, P., Browaeys, A., and Grangier, P. Quantum Logic via Optimal Control in Holographic Dipole Traps. *J. Opt. B 7* (2005), S341–S346.

[21] Dowling, J. P., and Milburn, G. Quantum Technology: The Second Quantum Revolution. *Phil. Trans. R. Soc. Lond. A 361* (2003), 1655–1674.

[22] Elliott, D. *Bilinear Control Systems: Matrices in Action*. Springer, London, 2009.

[23] Ernst, R. R., Bodenhausen, G., and Wokaun, A. *Principles of Nuclear Magnetic Resonance in One and Two Dimensions*. Clarendon Press, Oxford, 1987.

[24] Ettinger, M., Høyer, P., and Knill, E. The Quantum Query Complexity of the Hidden Subgroup Problem is Polynomial. *Inf. Process. Lett. 91* (2004), 43–48.

[25] Fahmy, A. F., Marx, R., Bermel, W., and Glaser, S. J. Thermal Equilibrium as an Initial State for Quantum Computation by NMR. *Phys. Rev. A 78* (2008), 022317.

[26] Feodorov, A., Steffen, L., Baur, M., da Silva, M. P., and Wallraff, A. Implementation of a Toffoli Gate with Superconducting Circuits. *Nature (London) 425* (2012), 170–172.

[27] Feynman, R. P. Simulating Physics with Computers. *Int. J. Theo. Phys. 21* (1982), 467–488.

[28] Feynman, R. P. *Feynman Lectures on Computation*. Perseus Books, Reading, MA., 1996.

[29] Fisher, R., Helmer, F., Glaser, S. J., Marquardt, F., and Schulte-Herbrüggen, T. Optimal Control of Circuit Quantum Electrodynamics in One and Two Dimensions. *Phys. Rev. B 81* (2010), 085328.

[30] Floether, F., de Fouquières, P., and Schirmer, S. Robust Quantum Gates for Systems Subject to Decoherence via Optimal Control: Markovian vs non-Markovian Dynamics . e-print: http://arXiv.org/pdf/1107.4358, 2012.

[31] García-Ripoll, J. J., Zoller, P., and Cirac, J. I. Speed-Optimized Two-Qubit Gates with Laser Coherent Control Techniques for Ion Trap Quantum Computing. *Phys. Rev. Lett. 91* (2003), 157901.

[32] García-Ripoll, J. J., Zoller, P., and Cirac, J. I. Coherent Control of Trapped Ions Using Off-Resonant Lasers. *Phys. Rev. A 71* (2005), 062309.

[33] Greiner, M., Mandel, O., Esslinger, T., Hänsch, T. W., and Bloch, I. Quantum Phase Transition from a Superfluid to a Mott Insulator in a Gas of Ultracold Atoms. *Nature (London) 415* (2002), 39–44.

[34] Helmer, F., Mariantoni, M., Fowler, A. G., von Delft, J., Solano, E., and Marquardt, F. Cavity Grid for Scalable Quantum Computation with Superconducting Circuits. *Europhys. Lett. 85* (2009), 50007.

[35] Hofheinz, M., Wang, H., Ansmann, M., Bialczak, R. C., Lucero, E., Neeley, M., O'Connell, A. D., Sank, D., Wenner, J., Martinis, J. M., and Cleland, A. N. Synthesizing Arbitrary Quantum States in a Superconducting Resonator. *Nature 459* (2009), 546–549.

[36] Jané, E., Vidal, G., Dür, W., Zoller, P., and Cirac, J. Simulation of Quantum Dynamics with Quantum Optical Systems. *Quant. Inf. Computation 3* (2003), 15–37.

[37] Jirari, H., and Pötz, W. Quantum Optimal Control Theory and Dynamic Coupling in the Spin-Boson Model. *Phys. Rev. A 74* (2006), 022306.

[38] Johanning, M., Varón, A. F., and Wunderlich, C. Quantum Simulations with Cold Trapped Ions. *J. Phys. B 42* (2009), 154009.

[39] Jordan, S., and Alagic, G. Approximating the Turaev-Viro Invariant of Mapping Tori Complete for One Clean Qubit. arXiv.org/1105.5100, 2011.

[40] Jordan, S., and Wocjan, P. Estimating Jones and HOMFLY Polynomials with One Clean Qubit. *Quant. Inf. Comput. 9* (2009), 0264–0289.

[41] Jozsa, R. Quantum Algorithms and the Fourier Transform. *Proc. R. Soc. A. 454* (1998), 323–337.

[42] Kauffman, L., and Lomonaco, S. Topological Quantum Computing and the Jones Polynomial . *Proc. SPIE 6244* (2006), 62440Z.

[43] Kauffman, L., and Lomonaco, S. A Three-Stranded Quantum Algorithm for the Jones Polynomial. *Proc. SPIE 6573* (2007), 65730T–1–65730T–13.

[44] Kauffman, L. H., and Lomonaco, S. J. *Mathematics of Quantum Computation and Quantum Technology*. Chapman & Hall/CRC, Boca Raton, FL, 2008, ch. Quantum Hidden Subgroup Problems: An Algorithmic Toolkit, pp. 3–46.

[45] Kauffman, L. H., and Lomonaco, S. J. *Mathematics of Quantum Computation and Quantum Technology*. Chapman & Hall/CRC, Boca Raton, FL, 2008, ch. Quantum Computing and Quantum Topology, pp. 409–514.

[46] Kempe, J., Bacon, D., Lidar, D. A., and Whaley, K. B. Theory of Decoherence-Free Fault-Tolerant Quantum Computing. *Phys. Rev. A 63* (2001), 042307.

[47] Khaneja, N., Luy, B., and Glaser, S. J. Boundary of Quantum Evolution under Decoherence. *Proc. Natl. Acad. Sci. USA 100* (2003), 13162–13166.

[48] Khaneja, N., Reiss, T., Kehlet, C., Schulte-Herbrüggen, T., and Glaser, S. J. Optimal Control of Coupled Spin Dynamics: Design of NMR Pulse Sequences by Gradient Ascent Algorithms. *J. Magn. Reson. 172* (2005), 296–305.

[49] Khodjasteh, K., and Viola, L. Dynamical Quantum Error Correction of Unitary Operations with Bounded Controls. *Phys. Rev. A 80* (2009), 032314.

[50] Khodjasteh, K., and Viola, L. Dynamically Error-Corrected Gates for Universal Quantum Computation. *Phys. Rev. Lett. 102* (2009), 080501.

[51] Kitaev, A. Y., Shen, A. H., and Vyalyi, M. N. *Classical and Quantum Computation*. American Mathematical Society, Providence, 2002.

[52] Knill, E., and Laflamme, R. Power of One-Bit Quantum Information. *Phys. Rev. Lett. 81* (1998), 5672–5675.

[53] Konnov, A. I., and Krotov, V. F. On the Global Methods of Successive Improvement of Controllable Processes. *Autom. Remote Control 60* (1999), 1427–. Russian original: *Avtom. Telemekh.* **1999**, 77–88.

[54] Krotov, V. F. *Global Methods in Optimal Control*. Marcel Dekker, New York, 1996.

[55] Krotov, V. F., and Feldman, I. N. Iteration Method of Solving the Problems of Optimal Control. *Eng. Cybern. 21* (1983), 123–130. Russian original: *Izv. Akad. Nauk. SSSR Tekh. Kibern.* **52** (1983), 162–167.

[56] Lanyon, B., Barbier, M., Almeida, M. P., Jennewein, T., Ralph, T., Resch, K. J., Pride, G. J., O'Brien, J. L., Gilchrist, A., and White, A. Simplifying Quantum Logic Using HigherDimensional Hilbert Spaces. *Nature Physics 5* (2009), 134–140.

[57] Lapert, M., Zhang, Y., Braun, M., Glaser, S., and Sugny, D. Geometric Versus Numerical Optimal Control of a Dissipative Spin 1/2 Particle. *Phys. Rev. A 82* (2010), 063418.

[58] Lapert, M., Zhang, Y., Braun, M., Glaser, S., and Sugny, D. Singular Extremals for the Time-Optimal Control of Dissipative Spin-1/2 Particles. *Phys. Rev. Lett. 104* (2010), 083001.

[59] Leibfried, D., Blatt, R., Monroe, C., and Wineland, D. Quantum Dynamics of Single Trapped Ions. *Rev. Mod. Phys. 75* (2003), 281–324.

[60] Levine, W. S., Ed. *The Control Handbook*. CRC Press, Boca Raton in cooperation with IEEE Press, 1996.

[61] Lloyd, S. Universal Quantum Simulators. *Science 273* (1996), 1073–1078.

[62] Machnes, S., Sander, U., Glaser, S. J., de Fouquières, P., Gruslys, A., Schirmer, S., and Schulte-Herbrüggen, T. Comparing, Optimising and Benchmarking Quantum Control Algorithms in a Unifying Programming Framework. *Phys. Rev. A 84* (2011), 022305.

[63] Marx, R., Fahmy, A. F., Kauffman, L., Lomonaco, S., Spörl, A., Pomplun, N., Schulte-Herbrüggen, T., Myers, J., and Glaser, S. J. Nuclear Magnetic Resonance Quantum Calculations of the Jones Polynomial. *Phys. Rev. A 81* (2010), 032319.

[64] Motzkoi, F., Gambetta, J. M., Merkel, S. T., and Wilhelm, F. K. Optimal Control Methods for Rapidly Time-Varying Hamiltonians. *Phys. Rev. A 84* (2011), 022307.

[65] Nielsen, N. C., Kehlet, C., Glaser, S. J., and Khaneja, N. *Encyclopedia of Nuclear Magnetic Resonance*. Wiley Sons, Chichester, 2010, ch. Optimal Control Methods in NMR Spectroscopy .

[66] Nigmatullin, R., and Schirmer, S. G. Implementation of Fault-Tolerant Quantum logic Gates via Optimal Control. *New J. Phys. 11* (2009), 105032.

[67] Palao, J. P., and Kosloff, R. Optimal Control Theory for Unitary Transformations. *Phys. Rev. A 68* (2003), 062308.

[68] Passante, G., Moussa, O., Ryan, C., and Laflamme, R. Experimental Approximation of the Jones Polynomial by One Quantum Bit. *Phys. Rev. Lett. 103* (2009), 250501.

[69] Peirce, A., Dahleh, M., and Rabitz, H. Optimal Control of Quantum Mechanical Systems: Existence, Numerical Approximations and Applications. *Phys. Rev. A 37* (1987), 4950–4962.

[70] Porras, D., and Cirac, J. I. Effective Quantum Spin Systems with Trapped Ions. *Phys. Rev. Lett. 92* (2004), 207901.

[71] Rebentrost, P., Serban, I., Schulte-Herbrüggen, T., and Wilhelm, F. K. Optimal Control of a Qubit Coupled to a Non-Markovian Environment. *Phys. Rev. Lett. 102* (2009), 090401.

[72] Sachdev, S. *Quantum Phase Transitions*. Cambridge University Press, Cambridge, 1999.

[73] Schulte-Herbrüggen, T., Spörl, A., Khaneja, N., and Glaser, S. J. Optimal Control for Generating Quantum Gates in Open Dissipative Systems. *J. Phys. B 44* (2011), 154013. for an early version see e-print: http://arXiv.org/pdf/quant-ph/0609037.

[74] Schulte-Herbrüggen, T., Spörl, A., Marx, R., Khaneja, N., Myers, J., Fahmy, A., and Glaser, S. *Lectures on Quantum Information*. Wiley-VCH, Weinheim, 2007, ch. Quantum Computing Implemented via Optimal Control: Theory and Application to Spin and Pseudo-Spin Systems, pp. 481–501.

[75] Schulte-Herbrüggen, T., Spörl, A. K., and Glaser, S. J. Quantum CISC Compilation by Optimal Control and Scalable Assembly of Complex Instruction Sets beyond Two-Qubit Gates. e-print: http://arXiv.org/pdf/0712.3227, 2007.

[76] Schulte-Herbrüggen, T., Spörl, A. K., Khaneja, N., and Glaser, S. J. Optimal Control-Based Efficient Synthesis of Building Blocks of Quantum Algorithms: A Perspective from Network Complexity towards Time Complexity. *Phys. Rev. A 72* (2005), 042331.

[77] Schulte-Herbrüggen, T., Spörl, A. K., Waldherr, K., Gradl, T., Glaser, S. J., and Huckle, T. *in: High-Performance Computing in Science and Engineering, Garching 2007*. Springer, Berlin, 2008, ch. Using the HLRB Cluster as Quantum CISC Compiler: Matrix Methods and Applications for Advanced Quantum Control by Gradient-Flow Algorithms on Parallel Clusters, pp. 517–533.

[78] Shor, P., and Jordan, S. Quantum Computing with Realistically Noisy Devices. *Quant. Inf. Comput. 8* (2008), 0681–0714.

[79] Shor, P. W. Algorithms for Quantum Computation: Discrete Logarithms and Factoring. In *Proceedings of the Symposium on the Foundations of Computer Science, 1994, Los Alamitos, California* (1994), IEEE Computer Society Press, New York, pp. 124–134.

[80] Shor, P. W. Polynomial-Time Algorithms for Prime Factorisation and Discrete Logarithm on a Quantum Computer. *SIAM J. Comput. 26* (1997), 1484–1509.

[81] Singer, K., Poschinger, U., Murphy, M., Ivanov, P., Ziesel, F., Calarco, T., and Schmidt-Kaler, F. Trapped Ions as Quantum Bits: Essential Numerical Tools. *Rev. Mod. Phys. 82* (2010), 2609.

[82] Sontag, E. *Mathematical Control Theory*. Springer, New York, 1998.
[83] Spörl, A. K., Schulte-Herbrüggen, T., Glaser, S. J., Bergholm, V., Storcz, M. J., Ferber, J., and Wilhelm, F. K. Optimal Control of Coupled Josephson Qubits. *Phys. Rev. A 75* (2007), 012302.
[84] Stojanović, V. M., Fedorov, A., Wallraff, A., and Bruder, C. Quantum-Control Approach to Realize a Toffoli Gate in Circuit QED. *Phys. Rev. B 85* (2012), 054504.
[85] Tannor, D. J., and Rice, S. A. Control of Selectivity of Chemical Reaction via Control of Wavepacket Evolution. *J. Chem. Phys. 83* (1985), 5013–5018.
[86] Wiseman, H. M., and Milburn, G. J. *Quantum Measurement and Control*. Cambridge University Press, Cambridge, 2009.
[87] Wunderlich, C. Quantum physics: Trapped Ion Set to Quiver. *Nature 463* (2010), 37–39.
[88] Xu, R., Yan, Y. J., Ohtsuki, Y., Fujimura, Y., and Rabitz, H. Optimal Control of Quantum Non-MarkovianDissipation: Reduced Liouville-Space Theory. *J. Chem. Phys. 120* (2004), 6600–6608.
[89] Yamamoto, T., Pashkin, Y. A., Astafiev, O., Nakamura, Y., and Tsai, J. S. Demonstration of Conditional Gate Operation Using Superconducting Charge Qubits. *Nature (London) 25* (2003), 941–944.
[90] Zanardi, P., and Rasetti, M. Noiseless Quantum Codes. *Phys. Rev. Lett. 79* (1997), 3306–3309.
[91] Zhang, Z., and Chen, G. *Mathematics of Quantum Computation and Quantum Technology*. Chapman & Hall/CRC, Boca Raton, FL, 2008, ch. Superconducting Quantum Computing Devices, pp. 171–222.
[92] As the number of strands in the braid representation of a knot determines the number of qubits needed to evaluate the Jones polynomial, avoid to evaluate links which contain circles *disjoint* from the rest of the link: then an easier quantum calculation can evaluate the Jones polynomial of the knot without disjoint circles. Finally, add n circles to the knot and multiply the Jones polynomial evaluated by $(-A^2 - A - 2)^n$.
[93] As the polarization in NMR ensembles is very low, a semiclassical description applies, in which phase sensitive detection (of -1-quantum coherences) is standard [23] without being in conflict with the non-commuting observables $\{\sigma_x, \sigma_y\}$.
[94] The problem actually roots in finding a viable protected subspace rather than drawing profit from it.